Precise and rapid distance measurements by scatterometry

doi: 10.1364/OE.20.003954

Precise and rapid distance measurements by scatterometry

Tetsuya Hoshino,[1,*] Toyohiko Yatagai,[2] and Masahide Itoh[1]

[1]*Institute of Applied Physics, University of Tsukuba, 1-1-1 Tennoudai, Tsukuba 305-8577, Japan*
[2]*Center for Optical Research and Education, Utsunomiya University, 7-1-2 Yoto, Utsunomiya, Tochigi 321-8585, Japan*
[*]*hoshino@gabor.bk.tsukuba.ac.jp*

Abstract: We found that the distances between isolated scatterers with similar columnar shapes could be measured by taking a single Fourier transform of their diffraction intensity. If the scatterers have different shapes, the distances between similar shapes can be selected from the distances between all the shapes. The distance from a specific scatterer can be measured with a resolution of 0.8 wavelengths and a precision of 0.01 wavelengths. This technique has the potential to be used in a novel optical memory that has a memory density as high as that of holographic memory, while can be fabricated by simple transfer molding. We used rigorous coupled-wave analysis to calculate the diffraction intensity. Some of the results were verified by nonstandard finite-difference time-domain simulations and experiments.

OCIS codes: (050.5745) Resonance domain; (070.2025) Discrete optical signal processing; (210.4680) Optical memories; (290.3700) Linewidth.

References and links

1. I. McNulty, J. Kirz, C. Jacobsen, E. H. Anderson, M. R. Howells, and D. P. Kern, "High-resolution imaging by Fourier transform x-ray holography," Science **256**(5059), 1009–1012 (1992).
2. J. Miao, T. Ishikawa, B. Johnson, E. H. Anderson, B. Lai, and K. O. Hodgson, "High resolution 3D x-ray diffraction microscopy," Phys. Rev. Lett. **89**(8), 088303 (2002).
3. D. E. Sayers, E. A. Stern, and F. W. Lytle, "New technique for investigating noncrystalline structures: Fourier analysis of the extended x-ray-absorption fine structure," Phys. Rev. Lett. **27**(18), 1204–1207 (1971).
4. Y. Takahashi, K. Hayashi, and E. Matsubara, "Complex X-ray holography," Phys. Rev. B **68**(5), 052103 (2003).
5. T. A. Germer, "Effect of line and trench profile variation on specular and diffuse reflectance from a periodic structure," J. Opt. Soc. Am. A **24**(3), 696–701 (2007).
6. P. Boher, J. Petit, T. Leroux, J. Foucher, Y. Desieres, J. Hazart, and P. Chaton, "Optical Fourier transform scatterometry for LER and LWR metrology," Proc. SPIE **5752**, 192–203 (2005).
7. P. J. van Heerden, "Theory of optical information storage in solids," Appl. Opt. **2**, 387–393 (1963).
8. B. Hill, "Some aspects of a large capacity holographic memory," Appl. Opt. **11**(1), 182–191 (1972).
9. M. Born and E. Wolf, *Principles of Optics: Electromagnetic Theory of Propagation, Interference and Diffraction of Light,* 7th ed. (Cambridge University Press, Cambridge, 1999).
10. J. Nakayama, ""Periodic fourier transform and its application to wave scattering from a finite periodic surface," IEICE Trans. Electron," E **83-C**, 481–487 (2000).
11. D. A. Pommet, M. G. Moharam, and E. B. Grann, "Limits of scalar diffraction theory for diffractive phase elements," J. Opt. Soc. Am. A **11**(6), 1827–1834 (1994).
12. E. N. Glytsis, "Two-dimensionally-periodic diffractive optical elements: limitations of scalar analysis," J. Opt. Soc. Am. A **19**(4), 702–715 (2002).
13. M. G. Moharam and T. K. Gaylord, "Diffraction analysis of dielectric surface-relief gratings," J. Opt. Soc. Am. A **72**(10), 1385–1392 (1982).
14. P. Zijlstra, J. W. M. Chon, and M. Gu, "Five-dimensional optical recording mediated by surface plasmons in gold nanorods," Nature **459**(7245), 410–413 (2009).
15. B. V. Johnson, G. A. McDermott, M. P. O'Neill, C. Pietrzyk, S. Spielman, and T. L. Wong, "Optical disc reader for reading multiple levels of pits on an optical disc," U. S. Patent 5,854,779 (1998).
16. J. Spronck, M. El-Husseini, L. Jabben, P. Overschie, D. Hobbelen, P. du Pau, H. Polinder, and J. van Eijk, "Mastering high-density optical disks: a new concept design," Assembly Autom. **24**(4), 406–415 (2004).
17. K. Tanaka, M. Hara, K. Tokuyama, K. Hirooka, K. Ishioka, A. Fukumoto, and K. Watanabe, "Improved performance in coaxial holographic data recording," Opt. Express **15**(24), 16196–16209 (2007).
18. J. A. Rajchman, "Promise of optical memories," J. Appl. Phys. **41**(3), 1376–1383 (1970).
19. M. G. Moharam, D. A. Pommet, E. B. Grann, and T. K. Gaylord, "Stable implementation of the rigorous coupled

#160956 - $15.00 USD Received 4 Jan 2012; accepted 27 Jan 2012; published 1 Feb 2012

wave analysis for surface-relief gratings: enhanced transmission matrix approach," J. Opt. Soc. Am. A **12**(5), 1077–1086 (1995).
20. J. B. Cole, "High accuracy nonstandard finite-difference time-domain algorithms for computational electromagnetics: applications to optics and photonics," in *Advances in the Applications of Nonstandard Finite Difference Schemes*, R. E. Mickens, ed. (World Scientific, Singapore, 2006), pp. 89–189.
21. S. Banerjee, "Nonstandard finite-difference time-domain algorithm: application to the design of subwavelength diffractive optical elements," Ph.D. thesis, Univ. of Tsukuba (2006).
22. T. Kashiwa, Y. Sendo, K. Taguchi, T. Ohtani, and Y. Kanai, "Phase velocity errors of the nonstandard FDTD method and comparison with other high-accuracy FDTD methods," IEEE Trans. Magn. **39**(4), 2125–2128 (2003).
23. T. Hoshino, S. Banerjee, J. B. Cole, M. Itoh, and T. Yatagai, "Shape analysis of wavelength-insensitive grating in the resonance domain," Opt. Commun. **284**(10-11), 2466–2472 (2011).
24. T. Hoshino, S. Banerjee, M. Itoh, and T. Yatagai, "Design of a wavelength independent grating in the resonance domain," Appl. Opt. **46**(32), 7942–7956 (2007).
25. T. Hoshino, S. Banerjee, M. Itoh, and T. Yatagai, "Diffraction pattern of triangular grating in the resonance domain," J. Opt. Soc. Am. A **26**(3), 715–722 (2009).
26. P. Lalanne and E. Silberstein, "Fourier-modal methods applied to waveguide computational problems," Opt. Lett. **25**(15), 1092–1094 (2000).
27. K. Hirayama, E. N. Glytsis, and T. K. Gaylord, "Rigorous electromagnetic analysis of diffraction by finite-number-of-periods gratings," J. Opt. Soc. Am. A **14**(4), 907–917 (1997).
28. L. Li, J. Chandezon, G. Granet, and J.-P. Plumey, "Rigorous and efficient grating-analysis method made easy for optical engineers," Appl. Opt. **38**(2), 304–313 (1999).
29. J. W. Goodman, *Introduction to Fourier Optics,* 3rd ed. (Roberts and Company Publishers, Greenwood Village USA, 2005).
30. M. Bickerstaff, T. Arivoli, P. Ryan, N. Weste, and D. Skellern, "A low power 50 mhz fft processor with cyclic extension and shaping filter," in "Proceedings of the ASP-DAC '98. Asia and South Pacific," (IEEE, Yokohama,Japan, 1998), pp. 335–336.
31. V. Kumar, *Introduction to Parallel Computing: Design and Analysis of Algorithms* (Benjamin/Cummings Pub.Co., Redwood City, 1994).

1. Introduction

Diffraction patterns analysis provides a nondestructive, noncontact, and rapid method for accurately determining distance and obtaining a considerable amount of information on shape and size of scatters. Diffraction patterns can be used to determine distance directly without calibration based on the diffraction angle. They can also be used for diffraction microscopy [1, 2], extended x-ray absorption fine-structure (EXAFS) spectroscopy [3, 4], scatterometry of circuit lines [5, 6], and holographic memory [7, 8]. A diffraction microscope has one of the highest resolutions of all optical measurement devices, EXAFS gives the precise distance between atoms, and scatterometry is indispensable in examining semiconductors in the production line.

The principle purpose of diffraction analysis is to evaluate the distance between two scatterers. When the scatterers have slit-like shapes, simple approximations such as Fraunhofer diffraction theory are applicable for analysis [9, 10]. Coherent light is diffracted by the two slits and the diffracted light interferes at a screen in the far field. Since, according to Fraunhofer diffraction theory, the diffraction intensity is periodic relative to the diffraction angle at the screen [9], a Fourier transform (FT) can be applied to obtain easily the distance. The FT gives the period, which corresponds to the distance between the scatterers. However, this method is not popular for distance measurements, because the diffraction angle θ should satisfy $\theta << 1$ for Fraunhofer diffraction theory to be valid. The resolution is several times worse under this condition than at larger diffraction angles since the amount of data for the FT decreases as the range of θ becomes narrower. Moreover, this method is applicable only to systems containing only two scatterers.

EXAFS and diffraction microscopy are also easy analysis methods because they employ a FT to determine distances. They use Fraunhofer theory or some other scalar theory to calculate distances between several scatterers by employing phase information in addition to intensity information. Because they require phase information, they can be used to analyze only certain kinds of samples, for example, those having a periodic structure [1–4]. Moreover, the processing time is long because it is necessary to perform many FTs.

In this study, we consider thick scatterers in two dimensions, rather than thin slits. We propose using FT analysis to calculate the distance between objects such as columns in the

#160956 - $15.00 USD Received 4 Jan 2012; accepted 27 Jan 2012; published 1 Feb 2012

light propagation direction and we use only the diffraction intensity to obtain rapid and precise measurement results.

For an array of columnar objects, wide-angle diffraction should be simulated using a vector theory [11, 12], rather than a scalar theory such as Fraunhofer diffraction theory. Rigorous coupled-wave analysis (RCWA) [13] can analyze scattering from wavelength-scale columns more accurately than Fraunhofer theory. The effect of polarization on the diffraction intensity is large in this size regime and RCWA can evaluate TE and TM modes separately. Consequently, RCWA is expected to give more accurate results in this regime. One of our aims is to realize a precision that exceeds the diffraction limit by performing rigorous calculations.

This analysis can be applied to memory since an array of columns can function as high-density optical memory. By creating multivalued memory based on distance measurements using the high precision of this method, it should be possible to realize high-density memory. Because convex scatterers can be regions of optical absorption or birefringence, this type of memory can have multiple colors [14], strengths [15], polarizations [14], and layers [14]. Like Blu-ray discs [16], it can be fabricated by molding, and can have a memory density several times higher than that of the bit array of Blu-ray discs, which is limited by the minimum spot size of the lens.

Another type of high-density memory is holographic memory, which has been attracting interest for recording due to its high density [8] and high data transfer rate [17]. The greatest difference between a hologram and the proposed memory is its structure: a hologram has a continuous structure, whereas the proposed memory has a discrete structure. While the proposed memory is similar to holographic memory in that it uses light interference [18], it differs in that it consists of discrete columns. This new memory stores information in terms of distance from a specific column, whereas holographic memory stores information as the continuously varying density of the polymer medium.

In this paper, for the first time, we calculate the diffraction intensity distribution of columnar scatterers and demonstrate that the distance can be accurately derived by performing a single FT of the scattering intensity. We also demonstrate that a novel high-density memory can be realized using this system.

2. Methods

2.1 Method for calculating the diffraction intensity

In the present study, the diffraction intensity is calculated by RWCA [13, 19], using the program *DiffractMOD*^{TM} 1.5 (RSoft Design Group, Ossining, NY, USA). RCWA can directly determine the far-field diffraction intensity for a periodic array of scatterers. Such a periodic structure has a high diffraction efficiency only at specific angles. Both Λ/λ and the incident angle determine the minimum matrix size in RCWA calculations and the actual matrix size depends on the number of harmonics. We obtained an appropriate number of harmonics by adding more than 10 to the minimum number so that the total transmission became stable against number of harmonics.

To verify the RCWA results, a combination of the nonstandard finite-difference time-domain (NS-FDTD) method [20] and the Helmholtz–Kirchhoff integral theorem has been used to calculate the far-field diffraction intensity [21]. The FDTD method can be used in calculations for isolated convex scatterers. First, the electric field near the scatterers is derived using the FDTD method. The diffraction intensity far from the scatterers is then derived by applying the Helmholtz–Kirchhoff integral theorem to the electric field. The NS-FDTD method is expected to calculate the electric field more precisely than the conventional FDTD method [22]. The calculation parameters for the NS-FDTD method are the same as those used in a previous study [23].

Both RCWA and the FDTD method are vector theories and they employ two equations: one for TE modes and the other for TM modes. Here, we mainly focus on the TE mode equation because it is easier to analyze the results for TE than for TM [13, 23].

#160956 - $15.00 USD Received 4 Jan 2012; accepted 27 Jan 2012; published 1 Feb 2012

We used two new methods to determine the distance between two convex scatterers from diffraction intensity measurements: one is based on the diffraction angle distribution and the other is based on the diffraction wavelength distribution.

2.2 Distance determined from diffraction intensity as a function of diffraction angle

Figure 1 shows two-dimensional scatterers. We consider rectangular or triangular scatterers on a plate. They could represent small beads in water or pigment regions in a clear resin. For simplicity, we model scatterers as rectangular or triangular structures on a plate. There are two regions with a single boundary between them. Region 1 is air and region 2 is the convex scatterer and the plate, which both have a refractive index of 1.5. The scatterers have a height d and a width v. The distance between the centers of the bases of the two scatterers is w. The light is incident at an angle of 0° and it is diffracted at an angle θ. It has a wavelength λ and is TE polarized. The TE mode has an electric field normal to the plane of the page in Fig. 1 [13].

In the first method, the FT is taken of the diffraction intensity as a function of sin θ. The peak position on the horizontal axis then corresponds to the distance between the scatterers. The need for equidistant data as a function of sin θ is one of the reasons why RCWA is useful. When RCWA is applied to periodic structures, it generates a periodic distribution of diffraction angles as a function of sin θ. Therefore, RCWA provides equidistant data as a function of sin θ, which is favorable for the FT.

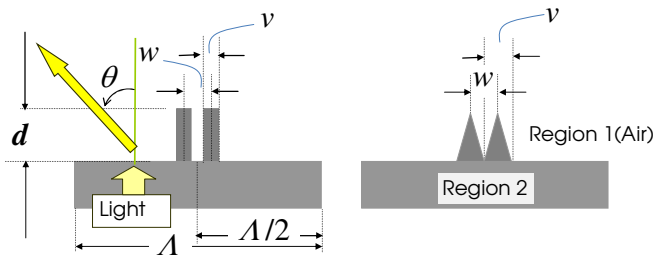

Fig. 1. Schematic diagram depicting arrangement of two convex scatterers. There is only one boundary between regions 1 and 2, which both extend to infinity. The plate and the scatterers have a refractive index n_2 of 1.5, while the refractive index of air n_1 is 1.0.

2.3 Distance determined from diffraction intensity as function of wavelength

In the second method, the FT is taken of the diffraction intensity as a function of $1/\lambda$ at a diffraction angle θ. $1/\lambda$ is varied between $1/\lambda_2$ and $1/\lambda_1$ ($\lambda_1 < \lambda_2$) in equal intervals and the sampling number for the diffraction intensity is N. The resulting horizontal axis is divided by $n_1 \sin\theta$. The extent of the horizontal data is then equal to $\{(N-1)/[n_1 \sin\theta\,(1/\lambda_1-1/\lambda_2)]\}$, and the range from 0 to half of this value is used for the analysis. Finally, the peak position on the horizontal axis provides the distance.

2.4 Experimental diffraction intensity for an infinite grating

Although the diffraction intensity is known to be periodic with respect to angle, it is not known whether it is periodic with respect to wavelength at large diffraction angles. It may be useful to confirm whether this is in fact the case. We therefore performed a simple experiment to measure the diffraction intensity as a function of wavelength. The sample used was an infinite triangular grating fabricated on a 2-mm-thick transparent acrylic plate. After UV curing the grating was removed from a metallic mold [24]. The grating had periods of 3 and 5 μm and $v/w = 1$ and $d/w = 0.48$. The grating period and profile were verified using atomic force microscopy (Nanopics 1000, Seiko Instruments, Inc.). The grating had a refractive index of 1.52. White light from a halogen lamp was collimated by a lens. The optical system consisted of (arranged in the following order) the lamp, a light guide, an iris diaphragm, two lenses, a 1-mm-diameter pinhole, and the sample. The collimated light was diffracted by the grating. The incident angle was 45°. The tip of an optical fiber was set 10 cm from the grating

#160956 - $15.00 USD Received 4 Jan 2012; accepted 27 Jan 2012; published 1 Feb 2012

to collect the diffracted light. Light diffracted at an angle of 0° was analyzed by an optical spectrum analyzer (HR2000, Ocean Optics) using an integration time of 100 ms. At each wavelength, the experimentally obtained intensity distribution was normalized by the light intensity passing through ground glass and the acrylic plate. Data processing was performed using code written in Matlab 6.1. The processing time was less than or equal to 20 ms for a computer with a 3.2 GHz CPU.

3. Results

3.1 Ability of RCWA to separate convex scatterers

Figure 2 shows two separate rectangular convex scatterers with $w/\lambda = 3$ and $v/\lambda = 1.5$. We first investigated the application of RCWA to these convexes. Although RCWA is generally only applicable to periodic structures, if Λ is sufficiently long, the diffraction pattern may corresponds to that of separate scatterers, so that RCWA can be used. As Λ increases, the ratio of the area of the plane region to that of the convex region increases and the number of higher-order diffractions also increases [9]. Both effects reduce the calculated diffraction efficiency by one diffraction order. In Fig. 2, the product of the diffraction efficiency calculated by RCWA and $(\Lambda/w)^2$ is plotted to negate these two effects. When $\Lambda/\lambda > 20$, the diffraction intensity is constant and it is assumed to equal that of two separate scatterers. At $\Lambda/\lambda = 6m$ ($m = 2, 3, 4, ...$), the data plotted in Fig. 2 exhibit valleys for $\theta = 9.6$, 30.0, and 56.4°. Diffraction from a periodic grating with $\Lambda/\lambda = 3$ does not have these diffraction angles, whereas diffraction from a periodic grating with $\Lambda/\lambda = 6$ does. When $\Lambda/\lambda = 6$ and $w/\lambda = 3$, Λ/λ for the grating will be 3. This may be why some diffraction angles for $\Lambda/\lambda = 6$ are missing. Fluctuations for $\theta = 9.6°$ and other angles can be prevented by selecting Λ/λ or the diffraction angle in the calculation.

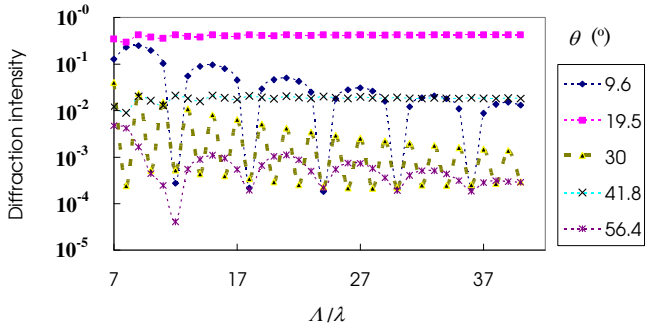

Fig. 2. Diffraction efficiency against Λ/λ for various θ ($w/\lambda = 3$, $v/\lambda = 1.5$, and $d/v = 2$).

3.2 Distance between two convexes

Figure 3(a) shows the calculated angular distribution of the diffraction intensity for two identical rectangles for $w = 3\lambda$. We first examined the effect of the convex size on diffraction. The scattering intensity does not vary monotonically with d when d and $v > 0.5\lambda$, whereas it increases proportionally with d^2 when d and $v < 0.2\lambda$. However, the convex size does not greatly affect the period of the variation in the diffraction. On the other hand, the diffraction intensity is periodic with respect to $\sin\theta$ and the period does not depend strongly on d. The period is obtained by taking the FT of the diffraction intensity in Fig. 3(a), as shown in Fig. 3(b). The intensity modulation by a single scatterer can be neglected here because its intensity (see Fig. 3(b)) is approximately 100 times smaller than that of two scatterers. Figure 3(b) shows that the peak position on the horizontal axis corresponds to the distance w/λ and that this axis can be expressed by w_{calc}/λ according to the above results. The angular periodicity may be caused by the same phenomenon that gives rise to Fraunhofer diffraction of a slit.

#160956 - $15.00 USD Received 4 Jan 2012; accepted 27 Jan 2012; published 1 Feb 2012

Figure 3 suggests that Fraunhofer diffraction occurs at both large and small diffraction angles for two rectangular scatterers with similar shapes and sizes.

We also performed the same calculation using the NS-FDTD method (see Fig. 3). Taking the FT gives the same w_{calc}/λ values as those obtained by RCWA (see Fig. 4). However, the FDTD method has a lower accuracy than RCWA, especially at low diffraction intensities. The FDTD method has an inherent error, which does not vanish when finer meshes are used in the calculation space; however, this error is reduced in the NS-FDTD method [22] more than the normal FDTD method. The FDTD method calculates only the near field; the far field is calculated based on the near-field data. Therefore, the error increases in the far field. The angular distribution of the diffraction intensity generated by two triangular scatterers was also calculated. Its envelope has a peak at about 45°, which seems to interrupt the periodic variation with w so that the modulation has a low periodicity.

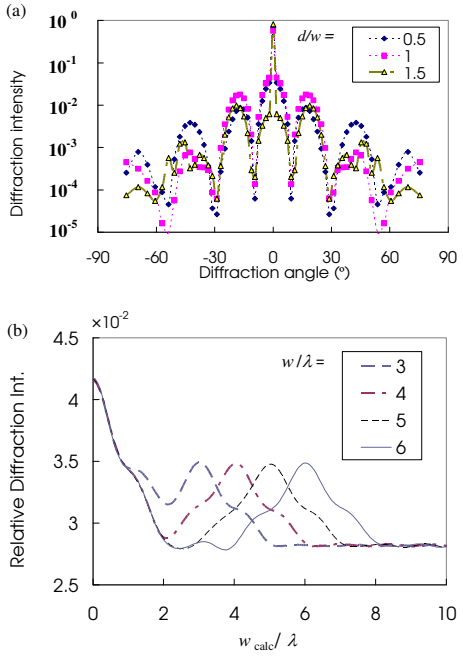

Fig. 3. (a) Diffraction intensity for two rectangles as a function of diffraction angle for various d/w (w/λ = 3, v/w = 0.5, and Λ/λ = 31). Auxiliary line that connects diffraction intensity is the envelope. (b) FT of diffraction intensity for various w/λ (v/w = 0.5, d/w = 0.5, and Λ/λ = 31).

#160956 - $15.00 USD Received 4 Jan 2012; accepted 27 Jan 2012; published 1 Feb 2012

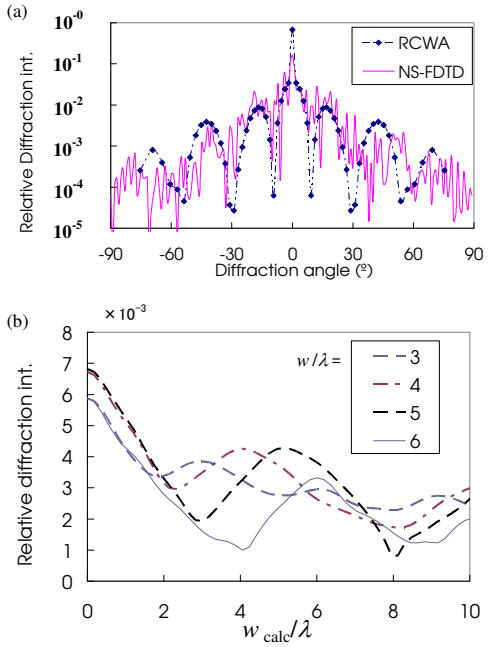

Fig. 4. Distance obtained from diffraction intensity by the NS-FDTD method as a function of diffraction angle. (a) Comparison of NS-FDTD and RCWA results for diffraction intensity from two rectangular scatterers as a function of diffraction angle ($w/\lambda = 3$, $v/w = 0.5$, $d/w = 0.5$, and $\Lambda/\lambda = 31$). Auxiliary line that connects diffraction intensity for RCWA is the envelope. (b) Result of FT of diffraction intensity by the NS-FDTD method for various w/λ ($v/w = 0.5$ and $d/w = 0.5$).

Figure 5(a) shows a plot of the calculated diffraction intensity from two triangular scatterers as a function of $1/\lambda$. It is clearly periodic. Figure 5(b) shows the FT of Fig. 5(a), with the horizontal axis scale divided by $n_1 \sin(\theta)$. Artificial fluctuations do not occur at angles of 19.5° and 47.2° (Fig. 2) and the same value of w_{calc}/λ is obtained at these angles. The peak position on the horizontal axis is equal to the distance w. A similar analysis can be performed for the same light path as that shown in Fig. 1, but for the opposite propagation direction. The diffraction intensity for rectangular scatterers as a function of $1/\lambda$ was also calculated, but it was not as periodic as that for triangular scatterers. The diffraction intensity fluctuation in Fig. 5(a) is periodic: not only does it have periodic local maxima and minima, but the periods have similar shapes. On the other hand, the shapes of the periods for the rectangular scatterers vary considerably. Only the maximum and minimum locations on the horizontal axis are periodic.

Figure 6 shows the diffraction intensity from triangular gratings with periods of 3 or 5 μm as a function of wavelength. The gratings are made of many pairs of two triangular scatteres. As is well known, the diffraction intensity from an infinite grating is a periodic function of angle if the grating produces higher-order diffractions. However, since its wavelength periodicity is not well known, we attempted to determine this experimentally. For the grating with $w = 5$ μm, the diffraction intensity varies periodically with $1/\lambda$. By taking the FT of the plotted data, the distance is estimated to be 5.1 μm. The deviation from the designed period may be due to limitations in the precision of the fabrication process and the optical system.

#160956 - $15.00 USD Received 4 Jan 2012; accepted 27 Jan 2012; published 1 Feb 2012

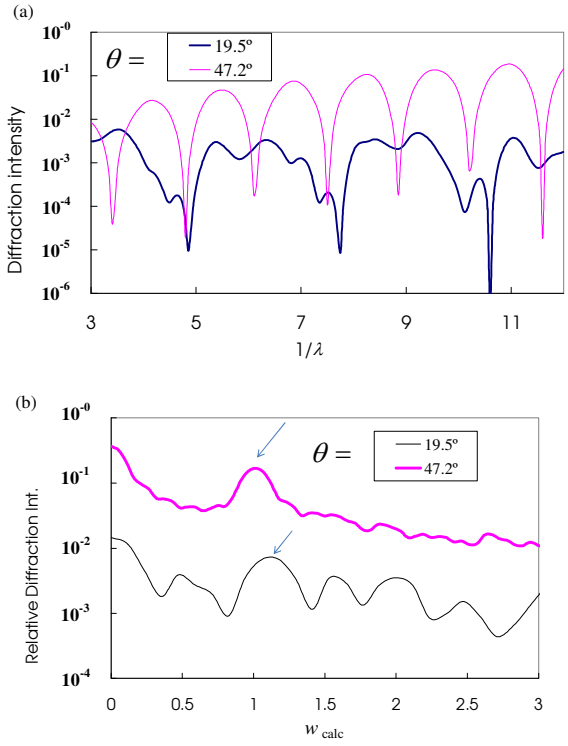

Fig. 5. Distance obtained from the FT of the diffraction intensity against $1/\lambda$. (a) Diffraction intensity for two triangular scatterers as a function of $1/\lambda$ for a specific angle θ (w = 1, v/w = 1, d/w = 1, and Λ = 30). (b) FT of (a).

#160956 - $15.00 USD
Received 4 Jan 2012; accepted 27 Jan 2012; published 1 Feb 2012

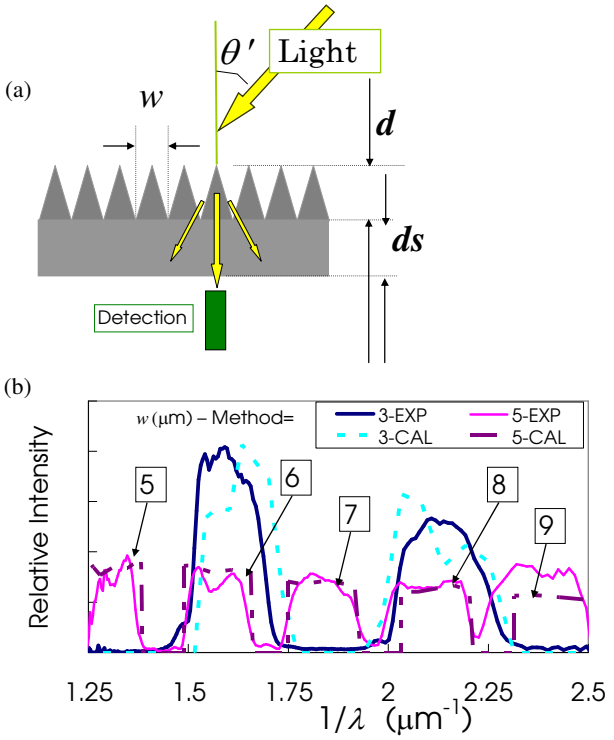

Fig. 6. Measured diffraction intensity for a triangular grating. (a) Schematic profile of the grating showing the definitions of w, d, and ds. Fill factor = 0.5 and aspect ratio d/w = 0.48; θ' is the incident angle. w is 3 or 5 μm. (b) Diffraction intensity from triangular gratings against $1/\lambda$ at a diffraction angle of 0° for grating periods of 3 and 5 μm. θ' is set to 45°, n_2 = 1.52, and ds = 2 mm. The numbers 5–9 denote the diffraction order of the grating with period 5 μm. "EXP" indicates the experimental results and "CAL" indicates the calculated results.

3.3 Effect of size difference

We also investigated the effect of using rectangular scatterers with different sizes to each other on the resulting w_{calc} for the configuration shown in Fig. 1. The size of one of the scatterers was increased without moving the center of its base and the distance between the two scatterers was kept constant. When the aspect ratio was kept constant and the size of one of the scatterers was varied by ±10%, the calculated distance deviated from the original value by as much as 8% when w/λ = 3, d/v = 1 for both scatterers, and v/λ = 1.5 for one scatterer. Similarly, the distance changed by 2% when w/λ = 6, d/v = 1 for both scatterers, and v/λ = 3 for one scatterer. Thus, varying the size of one of the scatterers alters the calculated distance w_{calc}. The distance derived by taking the FT deviates from its actual value by the difference in the widths or heights of the two scatterers. Therefore, conventional FT method such as that used in diffraction microscopy does not necessarily give an accurate distance. However, the distance can be accurately measured by using the method proposed in this paper.

3.4 Distances between more than two scatterers

We next performed measurements for more than two scatterers at one time. This leads to a shorter measurement time than for a single pair of scatterers and enables us to determine the distances in complex arrangements of scatterers. Moreover, if a specific shape is observed selectively, we can obtain information on the shape distribution.

In Fig. 7(a), the number and size of the rectangular scatterers are different from that in Fig. 1. The height of scatterer 1 is twice that of the others. Figure 7(b) show the FT of the

#160956 - $15.00 USD Received 4 Jan 2012; accepted 27 Jan 2012; published 1 Feb 2012

diffraction intensity as a function of diffraction angle for this pattern. The distances between scatterer 1 and scatterers 2, 3 and 4 are respectively 3λ, 4λ, and 5λ, and these distances give rise to strong peaks in the FT data. On the other hand, the distance between scatterers 2 and 4 is 2λ, and only a weak peak is observed. Thus, we can select the distance between two specific scatterers. The scattering intensity from a rectangular scatterer becomes stronger as d increases, which may give rise to the selectivity in this case.

This method can also detect variations in the height of the scatterers. We next investigated the effect of varying the height d of scatterers 2–4 of Fig. 7. For example, when d/λ for scatterer 3 was increased from 0.025 to 0.06 in 0.005 steps (i.e., 8 levels), its corresponding peak in the FT curve increased proportionately, with a correlation of $R^2 = 0.9997$, where R is the Pearson's product-moment correlation coefficient.

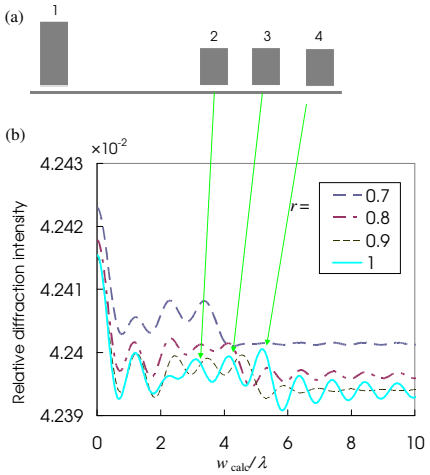

Fig. 7. (a) Rectangular scatterers with two different heights. r is the parameter which changes the distance between scatterers. The distance from scatterer 1 to the others is $3r\lambda$, $4r\lambda$, and $5r\lambda$. All v values are 0.2λ, d for scatterer 1 is 0.1λ, and d for the others is 0.05λ. $\Lambda/\lambda = 31$. (b) FT of angular distribution of diffraction intensity. The arrows indicate the peaks for scatterers 2, 3, and 4 in the case $r = 1$.

Figure 8(a) shows a collection of scatterers with different shapes and sizes, and Fig. 8(b) shows the corresponding FT of the diffraction intensity as a function of diffraction angle. Triangular scatterer 1 is twice the height and width of triangular scatterer 3 and sinusoidal scatterer 5. To identify the peaks in Fig. 8(b), individual calculations were carried out for only the two largest scatterers and their distance was determined. Thus, we can independently determine the distances between the individual scatterers shown in Fig. 8(a). Finally, the distances between two triangles and the triangle and the sine profile are selected from the distances between the five shapes. Thus, we can select the distance between specific triangles.

#160956 - $15.00 USD Received 4 Jan 2012; accepted 27 Jan 2012; published 1 Feb 2012

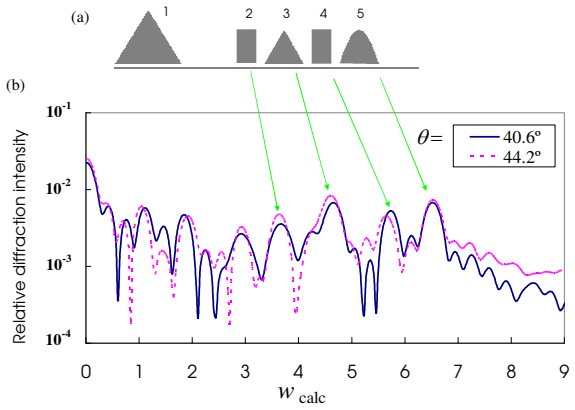

Fig. 8. Collection of scatterers with different shapes and sizes. (a) Array consisting of triangular, rectangular and sinusoidal scatterers. Distances between convex 1 and the other convexes are 3, 4, 5, and 6 from the left of the array. Λ = 43. v = 1 for scatterer 1, 0.5 for scatterers 3 and 5, and 0.25 for scatterers 2 and 4. d for scatterer 1 is 1, and for the others is 0.5. (b) FT of diffraction intensity for a specific angle θ. The arrows indicate the peaks associated with scatterers 2, 3, 4, and 5.

3.5 Resolution and precision

From Fig. 3(b), the precision of the calculated horizontal axis can be as small as 0.01λ when w_{calc}/w is used as the correction factor. When w was increased from 1 to 1.1 in steps of 0.01λ (with d/w = 0.25 and v/w = 0.5), w_{calc} was found to exhibit a linear dependence on w (R^2 = 0.9953). In Figs. 3 and 7, the precision is not strongly influenced by the wavelength of the refractive index dispersion, as w_{calc} depends on n_1 rather than n_2. n_1 is usually a refractive index of air.

The difference between the true distance w and w_{calc} was checked by increasing w/λ from 3 to 6, as shown in Fig. 3, and increasing w/λ from 3 to 5, as shown in Fig. 7. The average difference for these seven data points is 0.08λ, which is much smaller than the minimum spot size that can be achieved with the lens used (NA: 0.85). Additionally, the average difference for the TM mode is 0.09λ. Figure 7 shows that as the distance is reduced, peak splitting decreases and a resolution of 0.7–0.8λ is realized. The resolution is improved when a wider angular range is measured because the resolution for the FT improves when the data contains more cycles. For example, if θ is limited to the range –6° to + 6°, the precision may be 10 times worse than that of the case when θ is not limited. Fraunhofer diffraction theory is unsuitable in such a situation because it gives accurate results only when the diffraction angle is about 0°. This demonstrates the advantage of using RCWA, which can accurately estimate the diffraction intensity for a wide range of angles θ.

4. Discussion

4.1 Fraunhofer diffraction theory and RCWA

In Fraunhofer diffraction theory, the diffraction intensity from two slits depends on the diffraction angle and wavelength. The diffraction intensity from one slit is $A^2 w^2 \sin^2(\pi w\theta/\lambda)/(\pi w\theta/\lambda)^2$, while that from two slits is $2A^2\cos^2(\pi w\theta/\lambda)$, where A is a constant [9]. Here, the diffraction intensity is being observed at a point far from the midway of the two slits. The diffraction intensity is a periodic function of θ and $1/\lambda$ when $\theta << 1$. On the other hand, our results show that it is a periodic function of $\sin\theta$ and $1/\lambda$.

Fraunhofer diffraction theory is also useful for intuitively predicting the diffraction pattern. A single slit with an aperture width v has a diffraction pattern whose main peak width is proportional to the v/λ value of the scatterer. This is also applicable to an infinite triangular grating [25]. The width of the diffraction pattern envelope for a triangular grating is also

#160956 - $15.00 USD Received 4 Jan 2012; accepted 27 Jan 2012; published 1 Feb 2012

proportional to v/λ. Thus, Fraunhofer diffraction theory for a single slit can predict the diffraction pattern envelope for an infinite grating. If Λ is sufficiently large, an isolated triangular scatterer produces a certain diffraction pattern that approximates that of an infinite grating. In Fig. 2, we examined this situation for the two rectangular scatterers. As Λ increases, the diffraction pattern converges to a certain pattern. One reason for this convergence is that the interference from neighboring pairs of rectangular scatterers decreases. Another reason is that the number of higher-order diffractions increases with Λ, the number of data points increases, and the calculation produce a more accurate pattern.

As mentioned above, we find that RCWA is applicable if the calculation period is sufficiently long, although it is usually applied to periodic structures [26, 27]. RCWA and related methods [28] are faster and more accurate than others for far-field calculations [13]. For the first time, the diffraction intensity for a columnar shape was found to be periodic with respect to the diffraction angle or wavelength (see Figs. 3-6). Finally, a FT can easily convert diffraction data into distances (see Fig. 7). Using this method, we determined the distance from a specific column and also extracted shape-selective distances. This method requires measuring the diffraction intensity at normal incidence and over a wide diffraction angle range. The observed object can be an array of any kind of columns (e.g., biological cells or circuit patterns for IC chips).

4.2 Effect of shape

The shape dependence of the diffraction pattern was investigated by replacing a slit with a column with height. Figure 8 shows that a triangular scatterer can be distinguished from a rectangular one. The distances between triangular scatterers 1 and 3 and between triangular scatterer 1 and sinusoidal scatterer 5 could be selected.

The selectivity of the triangular scatterers from a mixture of triangular and rectangular ones shown in Fig. 8 may be due to three reasons. First, the angular distribution of the diffraction intensity for these shapes is different [23]. Second, the triangular scatterers have a stronger wavelength periodicity than the rectangular ones [23, 24]. The periodicity of the diffraction intensity for the triangular scatterers as a function of wavelength in Fig. 5 may be explained in terms of the main variable (w/λ). In contrast, the diffraction intensity for the rectangular scatterer in Fig. 5 is strongly affected by both w/λ and d/λ. Third, the intensity for the rectangular scatterers is weaker than that for the triangular scatterers at the observation angle. In Fig. 3(a), the rectangular scatterers have a weaker intensity at the observation angle and a weaker periodicity with respect to wavelength.

4.3 Comparison with holographic memory

The optical system proposed in this paper is similar to a holographic memory system. To read data, diffracted light is collimated by a lens and detected by a CCD detector [14]. Holographic memory has a high data transfer rate because the amount of data per transfer is large [14]. In columnar memory, it is necessary to read several distances simultaneously in order to achieve a high data transfer rate. For that purpose, the distance from a specific scatterer should be known. As shown in Fig. 7 and Fig. 8, this can be realized by enlarging the left-side scatterer in the array. Strong scattering from the enlarged scatterer masks the interference between the diffracted light from the other columns.

Columnar memory and holographic memory employ different schemes; their relationship is similar to that between the FT and inverse FT of an image [29]. According to Fraunhofer diffraction theory, the distance between two slits can be determined by performing a FT of the diffraction pattern. We can use an analogous idea to explain the mechanism of holographic memory and columnar memory. Columnar memory optically performs a FT of the distance and then an inverse FT to obtain the calculation results. In holographic memory, the distance is already the FT of the storage data and the inverse FT of the data is performed optically when it is read. Columnar memory can use all diffraction angles and its information is stored discretely in the storage medium, whereas holographic memory uses diffraction at specific angles and its information is stored continuously. The distance between scatterers in the

#160956 - $15.00 USD Received 4 Jan 2012; accepted 27 Jan 2012; published 1 Feb 2012

storage medium is significant in the former, whereas the distance between bright points in a diffraction pattern is significant in the latter.

4.4 Memory capacity and data transfer rate

The resolution and accuracy of the distance estimations are important considerations for memory and measurement applications since they determine the memory density and the scatterometry precision. According to the Nyquist–Shannon sampling theorem, if the sampling data for a parameter varies sinusoidally and there is sufficient data, the period of the sinusoidal curve can be rigorously determined. We obtained a precision of 0.01λ in the calculations (see section 3.5).

For memory such as that shown in Fig. 7(a), a storage capacity of 200 Gb (equivalent to that of a standard DVD disc) can be achieved if the distance can be measured to an accuracy of 0.01λ. When the value w/λ for one rectangular scatterer is increased from 3.8 to 4.11 in steps of 0.01, it produces 32 discrete values. In section 3.4, we showed that the height of a rectangle can be changed through eight levels. Using a combination of height and distance gives 256 different values. 256 is 2^8 and it requires eight rectangles on a DVD or Blu-ray disc. Therefore, the density of the memory shown in Fig. 7(a) can be eight times greater than a DVD or Blu-ray disc, if the same wavelength is used in the measurement. As a Blu-ray disc can store 25 Gb on a single side, the total storage capacity of the proposed memory is 200 Gb, which is comparable to that of a holographic memory disc. The shapes shown in Fig. 7(a) are simple and can be easily fabricated in a storage medium by transfer molding. This is an advantage over holographic memory, which requires a photosensitive medium for recording.

The long calculation time required for a FT limits the data transfer rate in this novel optical memory, and would need to be 10^6 times shorter to realize a data transfer rate as fast as standard Blu-ray discs. The time difference can be compensated by transferring a large amount of information per FT, using calculation hardware such as FFT chips [30], or by using parallel computing [31].

5. Conclusion

We found that the diffraction intensity without phase information enabled us to measure the distance between columnar scatterers by taking only one FT of the diffraction intensity as a function of wavelength or angle. Although this idea is similar to Fraunhofer diffraction theory for two slits, it is applicable to thick scatterers and also over a wide range of diffraction angles. It enables us to analyze the shape and measure the distance more accurately. We can determine the distances from a specific scatterer to other scatterers and the distance between selected shapes. An accuracy of 0.01λ can be realized if the shape and size are known.

Optical memory is a potential application of this concept. The memory density is as high as that of holographic memory, but the medium can be clear non-photosensitive plastic and fabrication can be simply carried out by transfer molding.

Acknowledgments

We thank Dr. J.B. Cole and Dr. S. Banerjee for allowing us to use NS-FDTD program. We also thank Dr. S. Aoki for discussing on this study's application to X-ray analysis.

#160956 - $15.00 USD Received 4 Jan 2012; accepted 27 Jan 2012; published 1 Feb 2012